Rotational temperatures of N2(C,0) and OH(A,0) as gas temperature estimates in the middle pressure Ar/O2 discharge

J Raud, M Laan, I Jõgi

Rotational temperatures of $N_2(C,0)$ and OH(A,0) as gas temperature estimates in the middle pressure Ar / O_2 discharge

J Raud[1], M Laan and I Jõgi
Institute of Physics, University of Tartu,
Tähe 4, 51010 Tartu, Estonia

E-mail: juri.raud@ut.ee

Abstract. Radiative transitions N_2(C-B,0-0) and OH(A-X,0-0) were used in order to estimate rotational temperatures of N_2(C,0) and OH(A,0) in the middle pressure Ar / 0.5% O_2 RF discharge. N_2(C,0) and OH(A,0) rotational temperature dependence on power density was determined and quenching / rotational relaxation frequencies of N_2(C,0) and OH(A,0) was calculated. It was found that at our conditions rotational temperature of OH(A,0) can be used for estimation of gas temperature while N_2(C,0) rotational temperature overestimates the gas temperature.
Classification numbers (PACS): 52.70.Kz, 52.80.Pi
Submitted to Journal of Physics D: Applied Physics

1. Introduction

Many plasma characteristics depend on the gas (translational) temperature, T_G. There are several T_G estimation methods e.g. by using pressure rise in closed systems due to temperature rise, by using thermocouples, spectral methods [1] etc. The gas temperature is frequently estimated on the basis of rotational temperature, T_{Rot}, of some molecules M* (e.g. N_2, N_2^+, OH, O_2, CO, CH etc. [2, 3]). However, this is possible only when some main conditions are fulfilled. First of all, the population of rotational states should follow the Boltzmann distribution. Besides, one of the next cases should be valid:

(1) the initial rotational population distribution (i.e. distribution just after the excitation) of M* corresponds to that equilibrium with T_G (hereafter: thermalized distribution). For example reaction, $He_m + N_2(X) \rightarrow He + N_2^+(B)$ produces a rotational population distribution of N_2^+(B,0) close to thermalized one [4, 5]. Here He_m stands for He metastable state atom.

(2) the initial rotational population distribution is non-thermalized but the lifetime of M* is longer than the time needed for the collisional relaxation to thermalized state. As a rule the condition holds better at higher pressures and smaller difference between the initial T_{Rot} and T_G.

Rotational temperatures $T_{Rot}(N_2)$ and T_{Rot}(OH), determined on the basis of spectra of N_2(C-B,0-0) and OH(A-X,0-0) transitions, are widely used for the estimation of gas temperature [6, 7, 8, 9 etc.]. We used these transitions to investigate the gas temperature of discharge in the argon-oxygen mixture at a low O_2 fraction. In similar mixtures non-thermalized or partly non-thermalized distribution of N_2(C,0) and/or OH(A,0) have been found [1, 10, 11, 12, 13 etc.]. Thus, it was not clear whether the calculated rotational temperatures characterize the gas temperature or not.

The aim of the study is to clarify whether $T_{Rot}(N_2)$ and T_{Rot}(OH) could be used as gas temperature estimates in the positive column region of the RF discharge in middle pressure Ar / 0.5% O_2 mixture.

[1] Author to whom any correspondence should be addressed.

For this purpose rotational spectra of N_2(C-B,0-0) and OH(A-X,0-0) transitions were recorded as a function of input power. On the basis of these measurements, the corresponding rotational temperatures were determined and quenching/rotational relaxation frequencies of excited states were calculated.

2. Set-up

Set-up is described in more details in [14].

Figure 1 presents a sketch of experimental device.

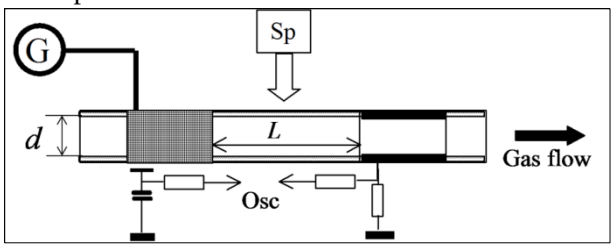

Figure 1. Experimental device. *G*- generator, *Osc*- oscilloscope, *Sp*- spectra recording position.

Ar / 0.5% O_2 plasma with and without N_2 addition was studied in quartz tube at pressure p=2 Torr and at gas flow rate 60 SCCM. The pressure was measured by using MKS Series 910 DualTrans Transducer. The flow of Ar and O_2 was set and maintained by mass flow controllers Alicat Scientific MC 16. A manual needle valve was used to dose N_2. The exact concentration of N_2 in the mixture remained undetermined but it was possible to estimate the upper limit of N_2 concentration comparing the pressure rises in the system caused by O_2 and N_2 flow. The residual pressure was ca $2\cdot10^{-2}$ Torr. When O_2 flow corresponding to 0.5% O_2 concentration was set, the pressure raised up to ca $5\cdot10^{-2}$ Torr, while in the case of N_2 flow the pressure raised up to ca $3\cdot10^{-2}$ Torr. Thus, the concentration of N_2 was smaller than 0.5%.

The bore diameter of the tube was d=6.5 mm. The discharge was excited with the generator of 40 MHz frequency and 100 W output power. The voltage was applied to the metal strap enveloping the tube. Another electrode, metal cylinder, was grounded and situated inside the tube. The distance between electrodes, L, was changeable but most of the experiments were carried out at the distance of L=80 mm. The electrical characteristics were recorded with oscilloscope TDS-540B. Spectra belonging to the positive column region of the discharge were recorded with spectrometers Ocean Optics 4000 and MDR-23 from lateral direction of the tube. Relative spectral sensitivity was determined by using Ocean Optics DH-2000-Cal calibrated light source. The temperature of the outer surface of the quartz tube was measured with the infrared thermometer Meterman IR608.

3. Results and discussion

3.1 Electrical characteristics

Electrical characteristics are described in more details in [14].

The equivalent circuit of electrical schema consisted from serially connected capacitor and plasma resistance. The capacitor consisted from the capacitance of quartz tube wall and near electrode space charge layer. Registered *i-u* curves and phase shift, φ, between *i* and *u* allowed to calculate the plasma voltage, $u_R = u\cdot\cos(\varphi)$.

Spectral measurements from different positions between electrodes showed that the intensity of spectral lines did not depend on the recording position. This indicated that electric field strength in the positive column, E_{PC}, was uniform. To determine E_{PC}, *i-u* curves and φ were recorded at different distances between powered and grounded electrodes (L = 40, 60 and 80 mm). At a constant current the voltage u_R grew linearly with the increase of distance between electrodes, L. The electric field strength E_{PC} was obtained from the slope of the dependence u_R = f(L). Electron temperature T_e and mobility were determined by taking OH(A,0) rotational temperature as a gas temperature and using code Bolsig+ [15]. Known mobility allowed to calculate electron concentration n_e. At our experimental

conditions E_{PC}=1-13 V/cm, $T_e \approx 4$ eV, $n_e \sim 10^{12}$ cm^{-3}. Current density was calculated as, $j = \frac{i}{S}$, where the cross-section, *S*, was taken equal to the inner cross-section of the quartz tube.

3.2 Spectral measurements

Figure 2 depicts spectra of Ar / 0.5% O_2 and Ar / 0.5% O_2 / N_2 recorded from the positive column region.

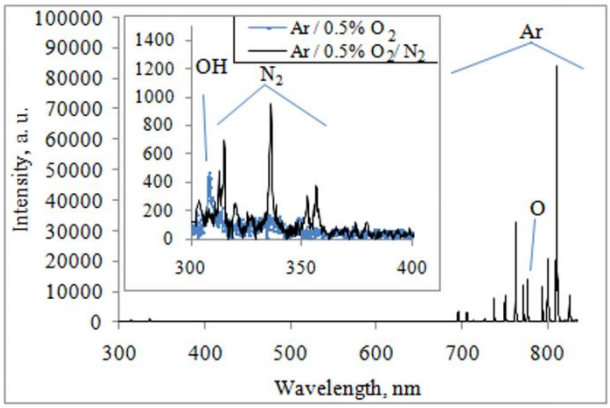

Figure 2. Spectrum of Ar / 0.5% O_2 / N_2. Inset: spectra of Ar / 0.5% O_2 and Ar / 0.5% O_2 / N_2 mixtures in wavelength range 300-400 nm. *i* =0.1 A.

The intensive spectral lines seen in figure 2 belonged to Ar and O. Weak band of trace gas OH(A-X) near 308 nm was also distinguishable in Ar / 0.5% O_2 mixture (figure 2 inset). The intensity of OH band was ca 200 times lower than the intensity of Ar 811.5 nm line. Addition of a small amount of N_2 caused the appearance of N_2(C-B) bands. Most intense N_2(C-B) bands belonged to the vibrational transitions 0-0 (bandhead at 337.1 nm), 1-0 (315.9 nm), 0-1 (357.7 nm) and 1-2 (353.7 nm). Intensity of bands N_2(C, $v \geq 2$) were very weak. The addition of N_2 did not influence the intensity of Ar lines but the intensity of OH band decreased.

3.3 Determination of rotational temperature

The rotational temperature was estimated comparing experimental spectrum and synthetic spectrum calculated for different temperatures assuming Boltzmann distribution of rotational states population. The temperature assuring the best fit between experimental and synthetic spectra was taken as rotational temperature. Apparatus function necessary for calculations of synthetic spectrum was measured by using a low pressure mercury lamp. The shape of spectral line fitted satisfactory with a Gaussian profile.

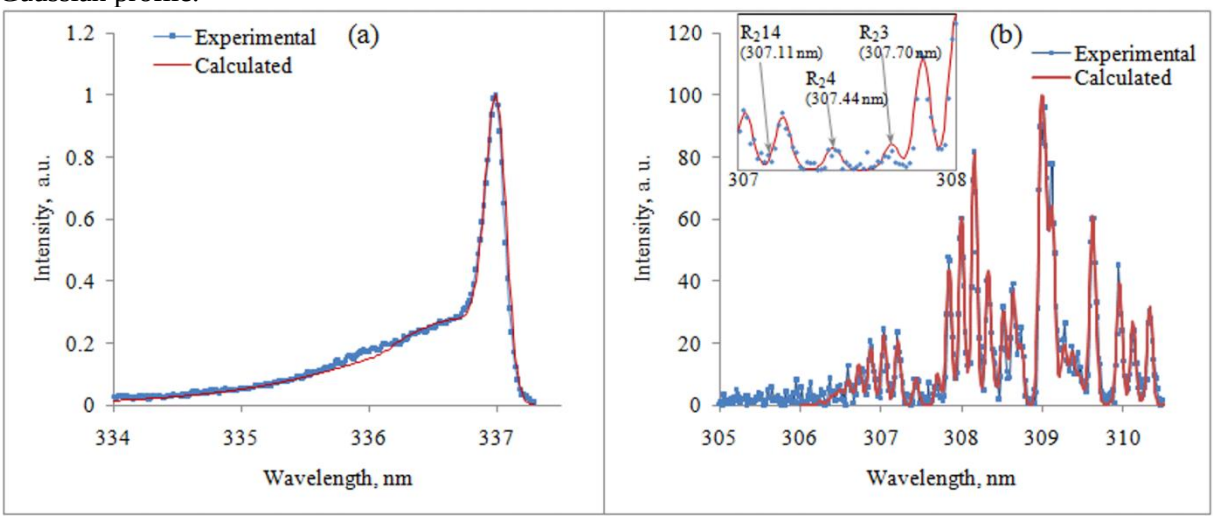

Figure 3. Measured and calculated rotational spectra.
(a): N_2(C-B, 0-0) transition; Ar / 0.5% O_2 / N_2; T_{Rot}=790 K; *i*=0.1A. Full-width at half maximum

$\Delta\lambda_{FWHM}$=0.105 nm.
(b): OH(A-X, 0-0) transition; Ar / 0.5% O_2; T_{Rot}=490 K; i=0.1 A. The peak correlation between experimental and synthetic spectra was 0.96. Inset: same spectrum in the wavelength range 307-308 nm. $\Delta\lambda_{FWHM}$=0.075 nm.

Rotational spectrum of N_2 (figure 3(a)) was calculated using data taken from [16]. For the calculation of synthetic spectrum the convolution integral of the apparatus function and the rotational spectrum was calculated. The best fit between synthetic and measured spectra was achived using the least square method. Because of the contribution of NH(A-X) weak emission at $\lambda \approx 336$ nm, the fitting was performed in spectral ranges 334.1 - 335.3 nm and 336.5 - 337.1 nm.
For the determination of OH(A, v=0) rotational temperature, the spectra comparison was carried out using code LIFBASE [17]. The spectrum of OH(A-X, 0-0) in wavelength region 305-311 nm is shown in the figure 3(b). As a rule, individual rotational lines were not resolved because of insufficient spectral resolution and each peak in spectrum represents a sum of overlapped rotational lines. An exception is demonstrated in the inset of figure 3(b) where individual lines of R_2 branch are distinguishable.
Figure 4 depicts $T_{Rot}(N_2)$ and T_{Rot}(OH), as a function of power density, $j{\cdot}E_{PC}$.

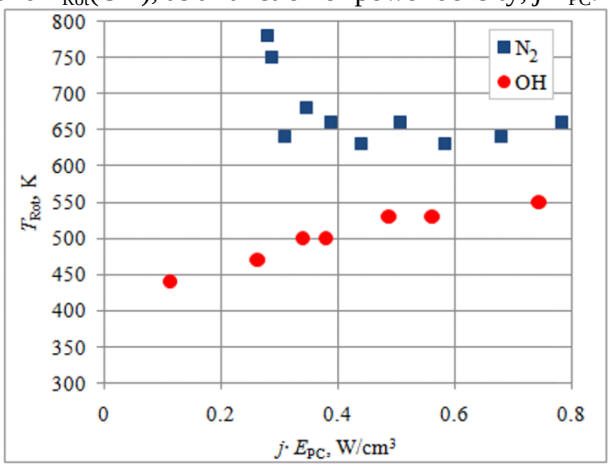

Figure 4. Rotational temperatures of N_2(C,0) and OH(A,0) as a function of power density.

$T_{Rot}(N_2)$ was higher than T_{Rot}(OH) in the whole range of power density values. T_{Rot}(OH) increased with the growing power density as expected, but the decrease of $T_{Rot}(N_2)$ at higher power densities suggested that $T_{Rot}(N_2)$ was not related to the gas temperature. It should be pointed that there was a linear dependence between T_{Rot}(OH) and the temperature at the outer surface of the tube whereas the correlation coefficient was 0.94. The same dependence in the case of $T_{Rot}(N_2)$ gave correlation coefficient 0.54.
In order to clarify the remarkable discrepancy of rotational temperatures it is essential to carry out a analysis of factors influencing N_2(C,0) and OH(A,0) rotational state populations.

3.4 Population of N_2(C,0) and OH(A,0) rotational states
Estimations given in this section are calculated by using following values: concentrations of electrons, Ar and O_2 are respectively $n_e=10^{12}$ cm^{-3}, $n_{Ar}=4{\cdot}10^{16}$ cm^{-3}, $n_{O2}=2{\cdot}10^{14}$ cm^{-3}, velocities of electrons and Ar atoms are respectively $v_e \approx 1{\cdot}10^6$ m·s^{-1}, $v_{Ar} \approx 5{\cdot}10^2$ m·s^{-1}. These values are characteristic to our experimental conditions.
In the stationary Ar / O_2 / N_2 discharge there are several mechanisms which could populate N_2(C) state e.g. stepwise electron impact excitation from lower N_2 states, pooling reactions from N_2(A), cascade population from higher energy levels of nitrogen molecule, energy transfer between N_2(X) and metastable Ar atoms, Ar_m and direct electron impact excitation from N_2 ground state. The latter mechanism produces N_2(C,0) at rotational temperature close to gas temperature [11].
As in our case the N_2 concentration was low, the population of N_2(C) by pooling reaction played a negligible role. The ground state and cascade paths of N_2(C) excitation are also not the main excitation routes as the electric field strength in the positive column in noble gases is considerably lower than

that in molecular gases [18]. The most probable $N_2(C)$ producing mechanism in our conditions is reaction

$$N_2(X, v=0) + Ar_m \rightarrow N_2(C, v \leq 3) + Ar \quad (1).$$

As a rule, the products of the reaction (1) are in vibrational states $v \leq 3$, whereas ca 80 % are in state v=0 ([19, 20]). We detected bands starting from the vibrational states v=0,1 of $N_2(C)$, other ones were very weak. According to [19, 21, 22], high rotational states of $N_2(C,0)$ are populated by reaction (1). Thus, $T_{Rot}(N_2)$ is close to T_G only in the case when the time constant of thermalization of $N_2(C,0)$ rotational states is shorter than the state lifetime. The lifetime of $N_2(C,0)$ state is determined by the radiative decay and by quenching in collisions with the host gas particles and electrons. Radiative decay frequency of $N_2(C,0)$ state is ca $2.4 \cdot 10^7 s^{-1}$ [23]. Using the cross-section $\sigma_{q\_e} \sim 10^{-15}$ cm^2 [10], the quenching frequency by electrons is $\nu_{q\_e} \sim 10^5$ s^{-1}. Quenching frequency of $N_2(C)$ by O_2 is only $\nu_{q\_O2} \approx 5 \cdot 10^4$ s^{-1} (rate coefficient k_{q_O2}=2.7·10^{-10}cm^{3}s^{-1}, [23]) and quenching frequency of $N_2(C)$ by Ar is even smaller, $\nu_{q\_Ar} \approx 10^4$ s^{-1} (k_{q_Ar}=3·10^{-13}cm^{3}s^{-1}, [24]). Because of low concentration, we can neglect the quenching by $N_2(X)$. Thus, in our experimental conditions the lifetime of $N_2(C,0)$ is mainly determined by the radiative lifetime.

The cross-section of $N_2(C,0)$ rotational relaxation by Ar is $\sigma_{Rel} \sim 10^{-15}$ cm^2 [25], thus frequency of relaxation in collisions with Ar is $\nu_{Rel} \approx 2 \cdot 10^6$ s^{-1} at our conditions.

As it has been concluded in [26], at low concentrations of H_2O in Ar, OH(A,0) is formed due to the collisions of H_2O with excited Ar atoms. In [27] a three-step reaction chain for OH(A) production was proposed. Collisions between H_2O and Ar_m, lead to the formation of H_2O in a Rydberg state:

$$H_2O + Ar_m \rightarrow H_2O(^3Ryd) + Ar(^1S) \quad (2)$$

Due to the collisions with Ar atoms $H_2O(^3Ryd)$ relaxes to lower states.

$$H_2O(^3Ryd) + Ar(^1S) \rightarrow H_2O(d^3A_1) + Ar(^1S) \quad (3)$$

And finally the dissociation takes place:

$$H_2O(d^3A_1) \rightarrow OH(A^2\Sigma^+) + H(^2S) \quad (4)$$

70% of OH(A) is produced in the vibrational state v=0, ca 25% - in the state v=1 and 5% - in the state v=2. Reaction (4) produces OH(A,0) at high rotational states [27].

In Ar / O_2 plasma OH(A) could be formed also via H_2O collisions with metastable O atoms, O_m:

$$O_m + H_2O \rightarrow 2OH(X) \quad (5) \text{ [28]}$$

$$OH(X) + e \rightarrow OH(A) + e \quad (6) \text{ [29]}$$

Reaction (5) produces OH(X,0) at high rotational states [28]. When the rotational relaxation of OH(X,0) is negligible then reaction (6) produces OH(A,0) also at high rotational states. In the case of OH(A,0), rotational states $N' \geq 23$ are mainly predissociated (predissociation frequency $\nu_{PD} \sim 10^7$ s^{-1}, [30]).

According to [6, 31] the lifetime of OH(A,0) depends mainly on radiative decay and quenching in collisions with Ar, O_2, H_2O. The frequency of OH(A) radiative decay is $\nu_{Rad} \approx 1.3 \cdot 10^6$ s^{-1}, [32], i.e. it is ca 20 times lower than that of $N_2(C)$. Quenching by collisions has considerably lower frequencies. The highest rate coefficient (k_{q_H2O}=5.9·10^{-10} cm^{3}s^{-1}, [31]), is obtained for quenching with H_2O, but even with the assumption that there was 1% of H_2O in the mixture, the quenching frequency is by one order of magnitude smaller than ν_{Rad}. The frequency of the quenching by O_2 is $\nu_{q\_O2} \approx 10^4$ s^{-1} (k_{q_O2}=5·10^{-11}cm^{3}s^{-1}, [33]), and by Ar, $\nu_{q\_Ar} \approx 4 \cdot 10^3$ s^{-1} (k_{q_Ar}=8.8·10^{-14}cm^{3}s^{-1}, [31]). Thus, the lifetime of OH(A,0) is also determined by the radiative decay.

Moutret et al. [7] estimated that the time constant of OH(A,0) rotational relaxation in Ar is 0.4 ns at p=760 Torr and T= 500 K. At our pressure and at the same temperature this gives, $\nu_{Rel} \approx 7 \cdot 10^6$ s^{-1}. By using cross-section $\sigma_{Rel} \approx 2 \cdot 10^{-15}$ cm^2 [34], the resulting rotational relaxation in our condition is lower: $\nu_{Rel} \approx 4 \cdot 10^6$ s^{-1}.

3.5 Rotational temperature as a measure of gas temperature

According to estimations given in section 3.4, the frequency of N_2(C,0) rotational relaxation is ca one order of magnitude smaller than the frequency of quenching. Thus, N_2(C,0) rotational distribution is close to that formed by reaction (1) and $T_{Rot}(N_2)$ does not characterize the gas temperature. Figure 4 demonstrates that the growth of $j \cdot E$ caused a fall of $T_{Rot}(N_2)$. The effect is explainable keeping in mind that the growth of $j \cdot E$ is accompanied with an increase of n_e. As in the low and middle pressure discharges electrons are dominant quenchers of Ar_m [35], the growth of $j \cdot E$ diminishes the contribution of reaction (1). We speculate that the relative importance of direct electron impact excitation from the N_2 ground state increases. As a result the N_2(C,0) rotational temperature becomes closer to the gas temperature and in our case it is falling with the growth of $j \cdot E$.

In section 3.4 it was found that the frequency of rotational relaxation of OH(A,0) is 3-5 times higher than the frequency of quenching. Thus, the rotational distribution of OH(A,0) should be close to the thermalized one. However, in several works (e.g. [12, 13]), where the rotational relaxation frequency was considerably higher than in our case, it has been found that OH(A,0) rotational population distribution is characterized by two values of T_{Rot}. A study of this phenomenon was carried out in [13], (p=760 Torr, glow discharge with a water electrode) in different media. It was found that T_{Rot}(OH) estimated on the basis of rotational states N'<13 was close to T_G while for N'>13 it was 2-3 times higher. Deviation from the thermalized distribution was explained with (a) non-thermalized initial distribution, (b) high rate of OH(A,0) quenching by H_2O which reduces effective lifetime of OH(A) and causes only partially thermalized distribution.

Regularities of our spectrum showed that OH(A,0) rotational temperature has only one value. Indeed, when the population of higher rotational states is remarkable, the rotational line $R_2$14 should appear in the spectrum presented in the inset of figure 3(b). However, $R_2$14 line was not detected whereas the transition probability for $R_2$14 is ca 5 times larger than the probabilities for $R_2$3 and $R_2$4 lines [36] which are presented in the spectrum. This finding is consistent with the calculations: for T_{Rot}=500 K the population of N'>10 rotational states does not exceed 1%. Thus, it indicates that in our case the distribution was thermalized. In comparison with [13] in our case the thermalization of OH(A,0) was more effective because of low H_2O concentration, therefore the quenching rate of OH(A) should be considerably lower. This explanation is confirmed by regularities in spectra: in our spectrum the intensity of OH band was ca 200 times lower than that of Ar lines while in study [13] OH band intensity was about 2 times higher than that of Ar.

4. Conclusion

It was found that independently of the input power, in Ar / 0.5% O_2 plasma the rotational temperature of N_2(C,0) state was remarkable higher than that of OH(A,0). Besides, the growth of the input power led to the decrease of N_2(C,0) rotational temperature. The analysis showed that N_2(C,0) was mainly excited via N_2(X) collisions with Ar metastable atoms which populate higher rotational states. As the lifetime of N_2(C) is short, the thermalization of rotational distribution did not take place and thus the N_2(C,0) rotational temperature differed from the gas temperature.

Similarly with the case of N_2(C,0), OH(A,0) was produced at high rotational states, but due to the longer lifetime of OH(A), there was enough time for thermalization. Therefore, in the middle pressure Ar / 0.5% O_2 plasma the rotational temperature of OH(A,0) state corresponded to the gas temperature considerably better than that of N_2(C,0) state. This conclusion was supported by the finding that with the growth of the input power the rotational temperature of OH(A,0) increased as is expected to be in the case of equality of gas and rotational temperatures.

Acknowledgment

The study is supported by Estonian Grant Foundation, grant No 7462.

References

[1] Alandri J, Diamy A M, Guillerme J M, Legrand J C and Ben-Aim R I 1989 *Appl. Spectrosc.* **43** 681-87

[2] Moon S Y and Choe W 2003 *Spectrochim. Acta, Part B* **58** 249-57

[3] Fleitz P A and Seliskar C J 1987 *Appl. Spectrosc.* **41** 679-82

[4] Belikov A E 1997 *Chem. Phys.* **215** 97-109
[5] Endoh M, Tsuji M and Nishimura Y 1983 *J. Chem. Phys.* **79** 5368-75
[6] Xiong Q, Nikiforov A Y, Lu X P and Leys C 2010 *J. Phys. D: Appl. Phys*. **43** 415201 (10pp)
[7] Motret O, Hibert C, Pellerin S and Pouvesle J M 2000 *J. Phys. D: Appl. Phys*. **33** 1493-8
[8] Wang Q, Koleva I, Donnelly V M and Economou D J 2005 *J. Phys. D: Appl. Phys*. **38** 1690-7
[9] Kim J H, Kim Y H, Choi Y H, Choe W, Choi J J and Hwang Y S 2003 *Surf. Coat. Technol.* **171** 211-5
[10] Wang Q, Doll F, Donnelly V M, Economou D J, Sadeghi N and Franz G F 2007 *J. Phys. D: Appl. Phys*. **40** 4202–11
[11] Xu L, Sadeghi N, Donnelly V M and Economou D J 2007 *J. Appl. Phys*. **101** 013304 1-9
[12] Bruggeman P, Schram D C, Kong M G and Leys C 2009 *Plasma Process. Polym*. **6** 751–62
[13] Verreycken T, Schram D C, Leys C and Bruggeman P 2010 *Plasma Sources Sci. Technol*. **19** 045004 9pp
[14] Laan M, Raud J, Hein K and Jõgi I *J. Phys. D: Appl. Phys*. (to be published)
[15] Available from http://www.siglo-kinema.com/bolsig.htm
[16] Naghizadeh-Kashani Y, Cressault Y and Gleizes A 2002 *J. Phys. D: Appl. Phys*. **35** 2925–34
[17] Luque J and Crosley D R 1999 "LIFBASE: Database and Spectral Simulation Program (Version 1.5)", SRI International Report MP 99-009
[18] Raizer Y P 1991 Gas Discharge Physics (Berlin: Springer)
[19] Nguyen T D and Sadeghi N 1983 *Chem. Phys*. **79** 4l-55
[20] Kirkici H, Bruno D, Preiss L and Schaefer G 1990 *J. Appl. Phys*. **67** 6041-4
[21] Sadeghi N and Nguyen T D 1977 *J. Physique Lett*. **38** 283-5
[22] Derouard J, Nguyen T D and Sadeghi N 1980 *J. Chem. Phys*. **72** 6698-705
[23] Valk F, Aints M, Paris P, Plank T, Maksimov J and Tamm A 2010 *J. Phys. D: Appl. Phys*. **43** 385202 (8pp)
[24] Brunin A N, Danilychev V A, Dolgikh V A, Kerimov O M, and Lobanov A N 1976 *Sov. J. Quantum Electron.* **6/11** 1275-9
[25] Dham A K, Meath W J, Jechow J W and McCourt F R W 2006 *J. Chem. Phys.* **124** 034308 1-23
[26] Morozov A, Krücken R, Ottenthal T, Ulrich A and Wieser J 2005 *Appl. Phys. Lett*. **86** 011502 1-3
[27] Tabayashi K and Shobatake K 1988 *J. Chem. Phys*. **88** 835-44
[28] Gericke K H and Comes F J 1982 *Chem. Phys*. **65** 113-21
[29] Riahi R, Teulet Ph, Ben Lakhadar Z and Gleizes A 2006 *Eur. Phys J. D* **40** 223-30
[30] Sutherland R A and Anderson R A 1973 *J. Chem. Phys.* **58** 1226-34
[31] Leblond J B, Collier F, Hoffbeck F and Cottin P 1981 *J. Chem. Phys.* **74** 6242-55
[32] Brophy J H, Silver J A and Kinsey J L 1974 *Chem. Phys. Lett.* **28** 418-21
[33] Tamura M, Berg P A, Harrington J E, Luque J, Jeffries J B, Smith G P and Crosley D R 1998 *Combust. Flame* **114** 502–14
[34] Lengel R K and Crosley D R 1977 *J. Chem. Phys*. **67** 2085-101
[35] Ferreira C M, Loureiro J and Ricard A 1985 *J. Appl. Phys.* **57** 82-90
[36] Dieke G H and Crosswhite H M 1962 *J. Quant. Spectr. Radiative Transfer* **2** 97-199